CHAPTER 20

Targeting of Reporter Molecules to Mitochondria to Measure Calcium, ATP, and pH

Anna M. Porcelli,[*] Paolo Pinton,[†] Edward K. Ainscow,[‡] Anna Chiesa,[§] Michela Rugolo,[*] Guy A. Rutter,[‡] and Rosario Rizzuto[§]

[*] Department of Biology
University of Bologna
40126 Bologna, Italy

[†] Department of Biomedical Sciences and C.N.R.
Center for the Study of Biomembranes
35121 Padova, Italy

[‡] Department of Biochemistry
University of Bristol
Bristol, BS8 1TD United Kingdom

[§] Department of Experimental and Diagnostic Medicine
Section of General Pathology
44100 Ferrara, Italy

METHODS IN CELL BIOLOGY, VOL. 65

I. Introduction

The study of isolated mitochondria, dating back to the 1960s, provided information on the biochemical routes that couple oxidation of substrates to the production of ATP. In this work, new concepts (such as the chemiosmotic mechanism of energy conservation, the import of proteins into mitochondria, and the existence of a mitochondrial genome with a different genetic code) became established dogmas of modern biology. At the same time, the availability of efficient probes and imaging systems allowed cell biologists to study mitochondria in living cells. These studies revealed that a variety of extracellular stimuli cause a rise in intracellular Ca^{2+} concentration of high spatiotemporal complexity, that in turn is decoded by intracellular effectors. Among these effectors are mitochondria that are endowed with a low-affinity transport system for Ca^{2+} and respond to microdomains of high Ca^{2+} generated in proximity to Ca^{2+} channels.

Recombinant reporter proteins containing mitochondrial targeting sequences are emerging as the tools of choice to study mitochondria in living cells. This chapter describes the development and use of protein chimeras targeted to either the mitochondrial matrix or intermembrane space. Aequorin, the first of the targeted recombinant probes, is a photoprotein of jellyfish of the genus *Aequorea* that emits light upon binding of Ca^{2+} to three high-affinity-binding sites. The second protein probe described in this chapter is luciferase. We discuss how the measurement of luciferase light emission *in situ* allows one to monitor the dynamics of ATP concentration changes in living cells. Finally, we describe use of variants of green fluorescent protein (GFP) as pH probes. GFP fluorescence is intense and resistant to photobleaching. Moreover, spectral variants of GFP have been developed for double or triple label and/or energy transfer experiments. As a result, GFP has emerged as the most widely employed probe for cell biologists and is used routinely to study protein sorting and trafficking, gene expression, and organelle structure and motility. For some applications, the pH sensitivity of GFP is a disadvantage. We describe how this property can be exploited to probe pH of mitochondria in living cells.

A. Targeting Strategy

Targeting a heterologous protein to mitochondria is now fairly straightforward. Indeed, apart from the 13 polypeptides encoded by mitochondrial DNA in humans, all

other mitochondrial proteins are encoded by nuclear genes. The signal peptides and routes allowing import of nuclear-encoded proteins into mitochondria have been investigated and clarified extensively in the past years. Therefore, while we describe targeting strategies for construction of our chimeric probes, it is obvious that similar, alternative approaches can be employed for developing novel chimeras.

1. Mitochondrial Matrix

To target heterologous reporter proteins to the mitochondrial matrix, we added at their N terminus the targeting sequence of the smallest subunit of human cytochrome *c* oxidase, COX8. This 44-amino acid (aa) COX subunit is encoded as a larger polypeptide, with a 25-aa-long N-terminal extension. This extension has the hallmarks of "mitochondrial presequences:" it is rich in basic and hydroxylated residues and devoid of acidic ones. In addition, it is recognized by the import machinery, triggering the transfer of the polypeptide to the matrix, and is then cleaved by resident proteases.

Figure 1A shows a generic map of a matrix-targeted recombinant probe. In all cases, an epitope tag is added to the coding region of the reporter protein, which allows for immunolocalization of the transfected protein. Indeed, our experience has been that matrix-targeted constructs are imported to the expected location, but it is always prudent, particularly with photoproteins (that cannot be directly visualized under the microscope), to confirm the appropriate sorting. In the chimeric construct, the cDNA encoding the epitope-tagged heterologous protein is fused in-frame downstream of a 150-bp fragment of the COX8 cDNA that encodes the first 33 aa of the mitochondrial precursor protein. The complete chimeric cDNA encodes, from the N to the C terminus: the 25-aa mitochondrial presequence, 8 aa of the mature COX8 protein, the 9-aa-long HA1 (hemagglutinin) tag, and the reporter protein of interest (aequorin, luciferase, or GFP mutant). Figure 1B shows the immunolocalization of one of these constructs (mitochondrially targeted aequorin, mtAEQ). The typical rod-like appearance of mitochondria can be easily appreciated.

2. Intermembrane Space (IMS)

The other target for novel probes was the outer surface of the ion-impermeable inner mitochondrial membrane. Indeed, although in equilibrium with the cytosol through the ion-permeable outer membrane, this region will contain local domains that differ in ion concentration from the bulk cytosol. In order to obtain the proper sorting and orientation across the inner mitochondrial membrane, we used the targeting sequence of glycerol phosphate dehydrogenase, an integral protein of the inner mitochondrial membrane with a large C-terminal portion protruding into the IMS. In chimeras destined for the intermembrane space, the reporter protein was fused to this C-terminal region (Fig. 2A). The immunolocalization shows that the protein chimeras are properly transported to the mitochondria (Fig. 2B). Localization of the chimera in the IMS cannot be determined by immunofluorescence, but can be deduced from the measurements carried out with the probe. In particular, the $[Ca^{2+}]$ changes revealed by the IMS-targeted chimera are not compatible with a matrix localization of the probe.

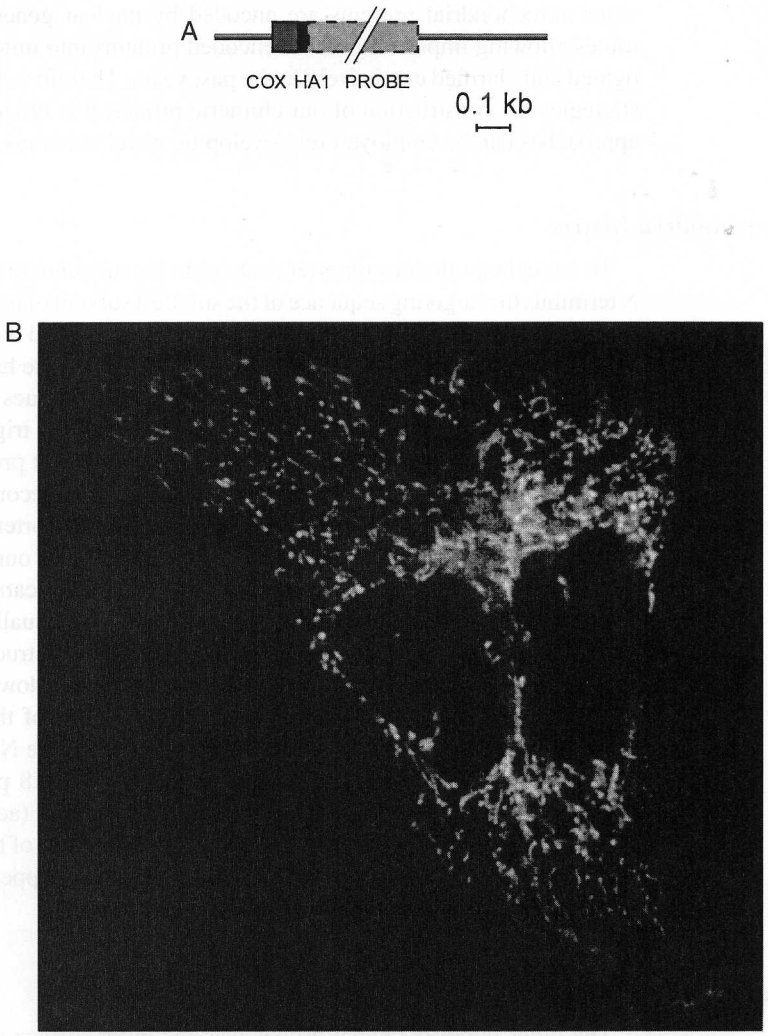

Fig. 1 (A) Generic map of a matrix-targeted recombinant probe. (B) Immunolocalization of mitochondrially targeted aequorin. Staining with a monoclonal antibody recognizing the hemagglutinin epitope (HA1) tag was detected with a TRITC-conjugated secondary antibody. The image, acquired on an inverted epifluorescence microscope, was captured with a back-illuminated CCD camera (Princeton Instruments) using the Metamorph software (Universal Imaging).

Rather, they are the response expected from a region in rapid equilibrium with the cytosol, but also sensing local domains of high [Ca^{2+}] generated at the surface of mitochondria by the release of Ca^{2+} from neighboring endoplasmic reticulum (ER) cisternae.

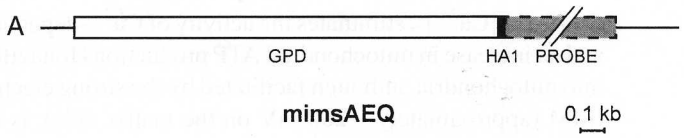

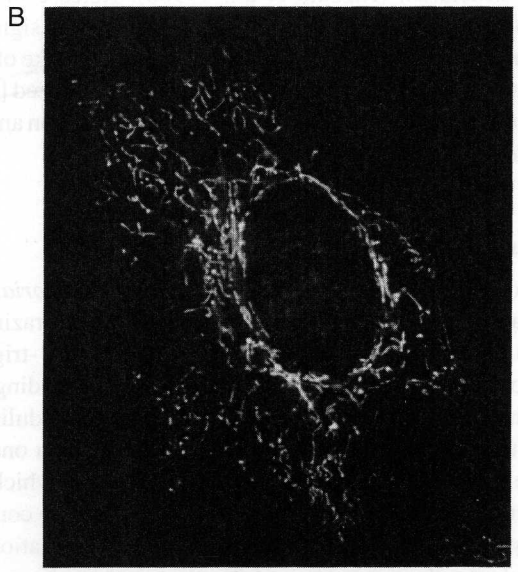

Fig. 2 (A) Schematic map of a reporter protein-glycerol phosphate dehydrogenase (GPD) targeted to the mitochondrial intermembrane space. (B) Immunolocalization of aequorin targeted to the mitochondrial intermembrane space (mimsAEQ), carried out as in Fig. 1.

II. Calcium

A. Mitochondria and Calcium Uptake: A Brief Overview

The outer and inner mitochondrial membranes (OMM and IMM, respectively) are markedly different, architecturally as well as functionally. It is noteworthy that the IMM is highly impermeable to ions in general, including Ca^{2+}. It has been demonstrated that upon physiological stimulation with agonists capable of generating inositol 1,4,5-triphosphate (InsP3) (Rizzuto *et al.,* 1993; Rutter *et al.,* 1993), a wide variety of cell types undergo major changes in mitochondrial matrix Ca^{2+} concentration ($[Ca^{2+}]_m$). In turn,

the rise in $[Ca^{2+}]_m$ stimulates the activity of Ca^{2+}-dependent enzymes of the Krebs cycle and an increase in mitochondrial ATP production (Jouaville *et al.,* 1999). Calcium uptake into mitochondria, although facilitated by the strong electrochemical potential across the IMM (approximately −200 mV on the matrix side), is dependent on the activity of a ruthenium red-sensitive electrogenic calcium uniporter. This Ca^{2+} uniporter exhibits a very low affinity ($K_m \sim 5-10\ \mu M$) for the cation (Carafoli, 1987; Gunter *et al.,* 1994; Pozzan *et al.,* 1994).

How do mitochondria accumulate Ca^{2+} given their low-affinity uptake system? The answer to this apparent paradox may reside in simple morphological details: in some regions of the cell the ER and mitochondria are in close proximity (<80 nm between the two structures) (Rizzuto *et al.,* 1998b). Release of Ca^{2+} from the ER at such a microdomain is sensed by adjacent mitochondria as a significant increase in cytoplasmic Ca^{2+} concentration ($[Ca^{2+}]_c$), which enables the uptake of Ca^{2+} by mitochondria, before the signal extends to the rest of the cytosol. The localized $[Ca^{2+}]_c$ then dissipates quickly, preventing excessive mitochondrial Ca^{2+} accumulation and collapse of the mitochondrial proton-motive force due to Ca^{2+} overload.

B. Mitochondrial Calcium Measurements Using Aequorin

Aequorin, isolated from the jellyfish *Aequorea victoria,* is composed of a 21-kDa apoprotein and a hydrophobic prosthetic group, coelenterazine (molecular mass ~400 Da). The two components must be associated for the Ca^{2+}-triggered light emission to occur. The holoprotein contains three high-affinity Ca^{2+}-binding sites (homologous to the sites present in other Ca^{2+}-binding proteins, such as calmodulin). Upon binding of Ca^{2+} ions, aequorin undergoes an irreversible reaction in which one photon is emitted (Fig. 3A). The rate of this reaction depends on the $[Ca^{2+}]$ to which the photoprotein is exposed. In particular, at $[Ca^{2+}]$ between 10^{-7} and $10^{-5}M$ (the concentration normally occurring in the cytoplasm of living cells), there is a direct relationship between $[Ca^{2+}]$ and the fractional rate of consumption of the photoprotein. Figure 3B shows the Ca^{2+} response curve of aequorin at physiological conditions of pH, temperature, and ionic strength. The fractional rate of aequorin consumption expressed as the ratio between the emission of light at a defined Ca^{2+} concentration (L) and the maximal rate of the light emission at saturating $[Ca^{2+}]$(L_{max}) is proportional to the second and third power of $[Ca^{2+}]$. This is the basis of the use of aequorin as a Ca^{2+} probe. Indeed, if all the light emitted by the photoprotein throughout an experiment, as well as that discharged at the end, is collected, it is possible to estimate L_{max} and then back-calculate the $[Ca^{2+}]$ to which the photoprotein was exposed at each point in time.

C. Advantages

1. Development of Targeted Probes

Prior to the isolation of the aequorin cDNA, the use of aequorin was limited to the cell types in which the photoprotein could be microinjected. Now it is possible not

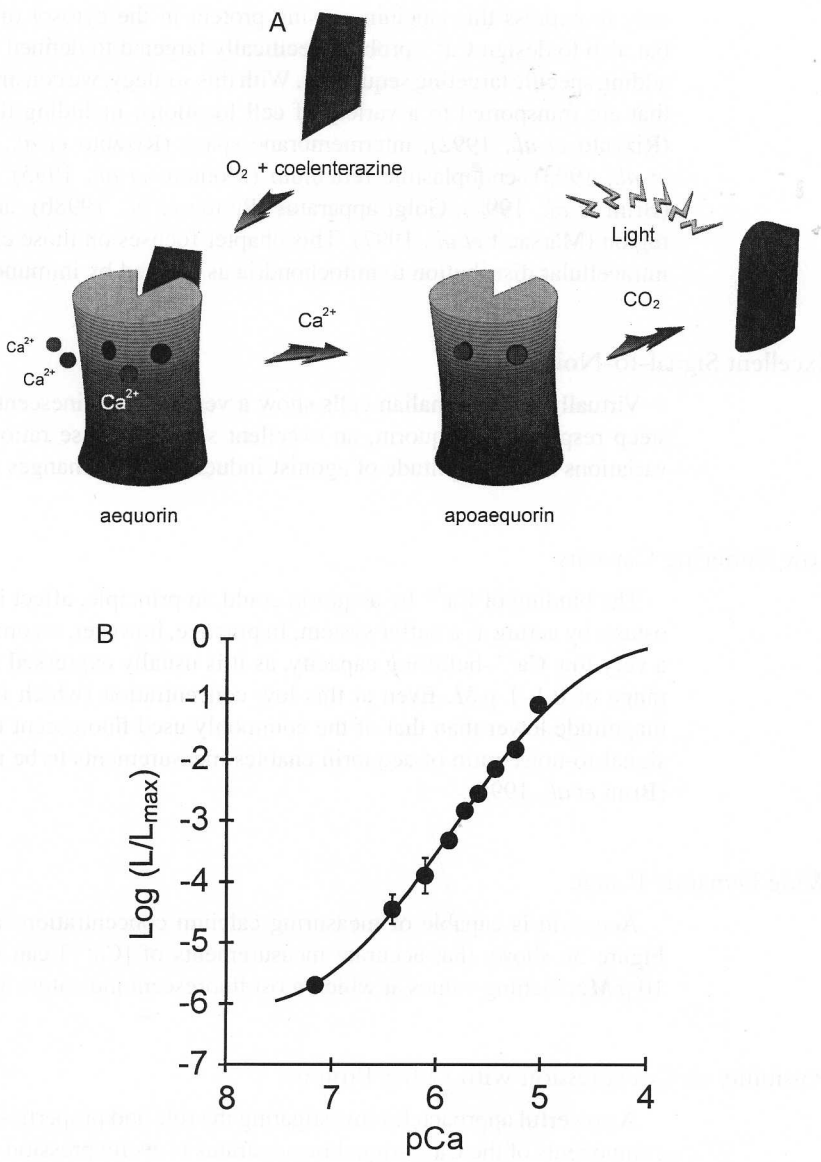

Fig. 3 (A) Schematic representation of the Ca^{2+}-dependent photon emission of aequorin. The functional probe is generated from the apoaequorin moiety (synthesized by the cell) and coelenterazine (imported from the surrounding medium). Binding of Ca^{2+} ions liberates the prosthetic group, with concomitant light emission and irreversible discharge of a molecule of aequorin. (B) Relationship between calcium concentration and light emission rate by active aequorin (L and L_{max} are, respectively, the instant and maximal rates of light emission). Note the direct relationship at calcium concentrations between 10^{-5} and $10^{-7}M$.

only to express this calcium-sensing protein in the cytosol of a variety of cell types, but also to design Ca^{2+} probes specifically targeted to defined subcellular locations by adding specific targeting sequences. With this strategy, we constructed aequorin chimeras that are transported to a variety of cell locations, including the mitochondrial matrix (Rizzuto *et al.,* 1992), intermembrane space (Rizzuto *et al.,* 1998b), nucleus (Brini *et al.,* 1993), endoplasmic reticulum (Montero *et al.,* 1995), sarcoplasmic reticulum (Brini *et al.,* 1997), Golgi apparatus (Pinton *et al.,* 1998b), and subplasmamembrane region (Marsault *et al.,* 1997). This chapter focuses on those chimeras with a selective intracellular distribution to mitochondria as verified by immunocytochemistry.

2. Excellent Signal-to-Noise Ratio

Virtually all mammalian cells show a very dim luminescent background. Given the steep response of aequorin, an excellent signal-to-noise ratio is obtained, and minor variations in the amplitude of agonist-induced $[Ca^{2+}]$ changes can be detected easily.

3. Low Buffering Capacity

The binding of Ca^{2+} by aequorin could, in principle, affect intracellular Ca^{2+} homeostasis by acting as a buffer system. In practice, however, recombinant aequorin exhibits a very low Ca^{2+}-buffering capacity, as it is usually expressed at a concentration in the range of 0.1–1 μM. Even at this low concentration (which is two to three orders of magnitude lower than that of the commonly used fluorescent indicators), the excellent signal-to-noise ratio of aequorin enables measurements to be made in cell populations (Brini *et al.,* 1995).

4. Wide Dynamic Range

Aequorin is capable of measuring calcium concentrations across a wide spectrum. Figure 3b shows that accurate measurements of $[Ca^{2+}]$ can be obtained from 0.5 to 10 μM, reaching values at which most fluorescent indicators are already saturated.

5. Possibility of Coexpression with Other Proteins

A powerful approach for investigating the role and properties of the various molecular components of the Ca^{2+}-signaling apparatus is overexpression of the protein of interest, and analysis of possible effects on intracellular calcium in the molecularly modified cell.

D. Disadvantages

1. Low-Light Emission

In contrast to some fluorescent dyes that emit up to 10^4 photons without photobleaching, only 1 photon can be emitted by an aequorin molecule. Moreover, the principle

of the use of aequorin for Ca^{2+} measurements is that only a small fraction of the total pool emits its photon every second. This is not a major limitation in population studies; conversely, single cell imaging requires very high expression and special apparatuses (Rutter *et al.,* 1996).

2. Expression May Be Inefficient and/or Slow

In the case of recombinant aequorin, transfection is the simplest loading procedure. A wide range of procedures have been developed, including calcium phosphate, liposomes, electroporation, and the gene gun. Nonetheless, some cell lines are resistant to transfection. Moreover, expression of recombinant aequorin may be inefficient. As a result, time for protein expression must elapse before Ca^{2+} measurements are carried out.

3. Overestimation of Average Value in a Nonhomogeneous Environment

The slope of the Ca^{2+} response curve of aequorin is steep. Therefore, if the increase of the $[Ca^{2+}]$ is not homogeneous, the average estimate will be biased toward the highest values.

E. Procedure

We obtained good aequorin expression in a wide variety of cell types (e.g., HeLa, CHO, COS, neurons, myocytes). In all cases, the cells are seeded on circular glass coverslips (13 mm in diameter) and allowed to grow until about 50% confluency. Cells are then transfected with 4 μg of mitochondrially targeted aequorin (mtAEQ) or 0.5 μg of mitochondrial intermembrane space (mims)AEQ using the calcium phosphate procedure. We noticed that high levels of mimAEQ expression had deleterious effects on some transfected cell populations. This problem was solved by reducing the quantity of DNA used for the transfection procedure. After 36 h, aequorin is reconstituted by adding the prosthetic group to the incubation medium [5 μ*M* coelenterazine for 2 h in DMEM supplemented with 1% fetal calf serum (FCS) at 37°C in 5% CO_2 atmosphere]. Approximately 2 h after reconstitution, cells are washed and transferred to the perfusion chamber of the measuring system. They are then perfused with KRB saline solution (Krebs–Ringer modified buffer: 125 m*M* NaCl, 5 m*M* KCl, 1 m*M* Na_3PO_4, 1 m*M* $MgSO_4$, 5.5 m*M* glucose, 20 m*M* HEPES, pH 7.4, 37°C).

The schematic representation of the measuring system is depicted in Fig. 4. In this system, the perfusion chamber, on top of a hollow cylinder, thermostatted by water jacket, is perfused continuously with buffer via a peristaltic pump; agonists and drugs are added to the same medium. The cell coverslip is placed a few millimeters from the surface of a low noise phototube. The photomultiplier is kept in a dark box maintained at 4°C. An amplifier discriminator is built in the photomultiplier housing. The pulses generated by the discriminator are captured by a Thorn EMI photon counting board, installed in an

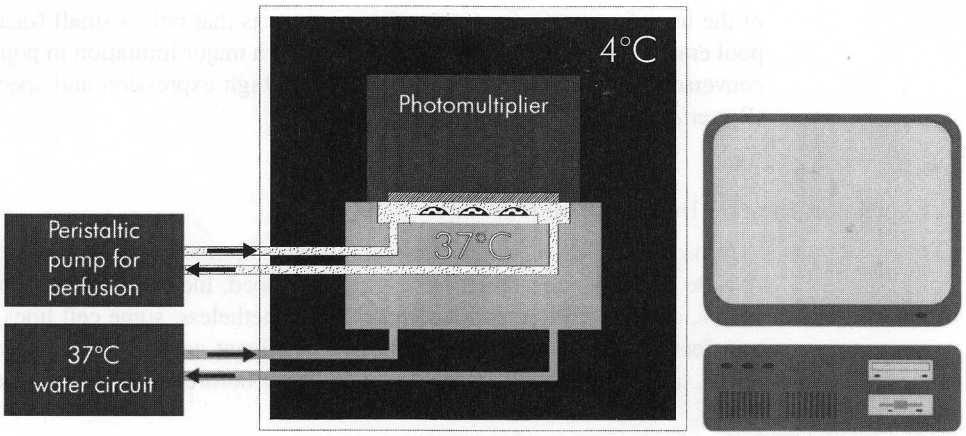

Fig. 4 Schematic representation of a custom-built luminometer. Cells loaded with a functional aequorin probe are incubated in a perfusion chamber at 37°C in close proximity to a photon-counting tube. The complete assembly is kept at 4°C, in the dark, to minimize extraneous signals. Acquisition of data and subsequent calculations to transform light emission into $[Ca^{2+}]$ are performed by a computer algorithm.

IBM-compatible computer. The board allows storage of data in the computer memory for further analysis.

An algorithm has been developed to calibrate the crude luminescent signal in terms of $[Ca^{2+}]$ that takes into account the instantaneous rate of photon emission and the total number of photons that can be emitted by aequorin in the sample (Brini *et al.*, 1995). To obtain the latter value, cells are lysed at the end of each experiment by perfusion with hypo-osmotic medium containing 10 m*M* $CaCl_2$ and a detergent (100 μ*M* digitonin). This perfusion discharges all aequorin that was not consumed during the experiment.

F. Results

Some typical results of $[Ca^{2+}]_m$ monitoring are shown in Figs. 5 and 6. In these experiments, HeLa cells expressing the appropriate aequorin chimera were stimulated with an agonist, histamine (100 μ*M*), which acts on a receptor coupled to the generation of inositol 1,4,5,-triphosphate and causes release of Ca^{2+} from intracellular stores.

The biphasic kinetics of $[Ca^{2+}]_c$ in HeLa cells transfected with unmodified aequorin (which is cytosolic) after stimulation with histamine is shown in Fig. 5. The release of Ca^{2+} from the stores causes an initially rapid, but temporary, increase in $[Ca^{2+}]_c$, to values of approximately 2.5 μ*M*, followed by a sustained increase in $[Ca^{2+}]_c$ above normal basal levels, which is maintained throughout the stimulation period.

Figure 5 shows measurements obtained in HeLa cells transiently expressing mtAEQ. Upon stimulation with histamine, there is a rapid increase in $[Ca^{2+}]_m$ to approximately 10 μ*M*, after which there is an equally rapid decrease to basal values. Given the targeting signal, it is expected that this chimeric protein is localized in the mitochondrial matrix.

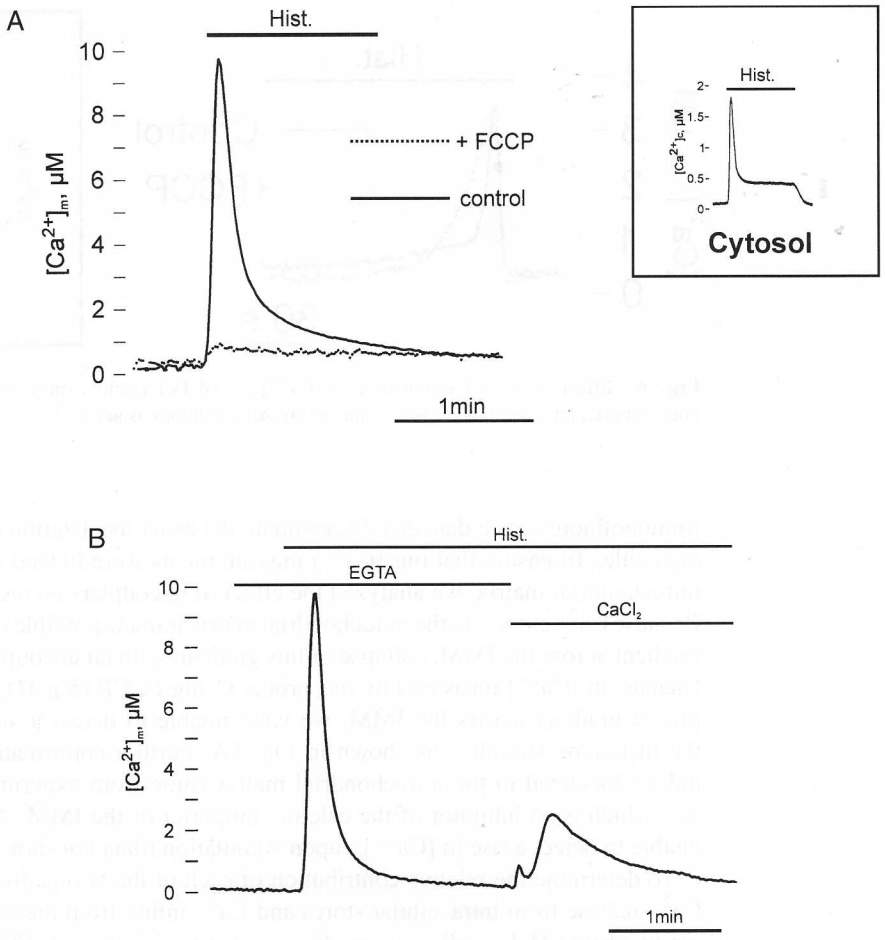

Fig. 5 (A) Effect of agonist stimulation on $[Ca^{2+}]_m$ of HeLa cells expressing aequorin targeted to the mitochondrial matrix (mtAEQ). After reconstitution of the photoprotein, coverslips with the cells were transferred to the thermostatted (37°C) chamber of the luminometer and perfused with modified Krebs–Ringer buffer (KRB; 125 m*M* NaCl, 5 m*M* KCl, 1 m*M* Na_3PO_4, 1 m*M* $MgSO_4$, 5.5 m*M* glucose, 20 m*M* HEPES, pH 7.4, 37°C). Where indicated, the cells were treated with 100 μ*M* histamine (Hist.) and/or with 5 μ*M* carbonylcyanide *p*-(trifuoromethoxy) phenylhydrazone (FCCP), added to KRB. In this and the following aequorin experiments, the traces are representative of at least five experiments. (B) The effect of release of Ca^{2+} from intracellular stores and Ca^{2+} influx on $[Ca^{2+}]_m$. Where indicated (EGTA), the cells were washed with 100 μ*M* EGTA and then treated with 100 μ*M* histamine (Hist.) added to KRB/EGTA. The medium was then switched with KRB (with 1 m*M* $CaCl_2$) and, where indicated (Hist.), the cells were challenged with 100 μ*M* histamine (added to KRB).

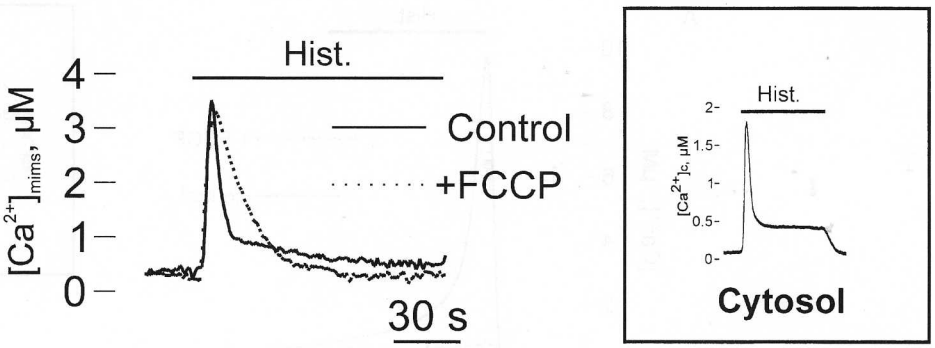

Fig. 6 Effect of agonist stimulation on $[Ca^{2+}]_{mims}$ of HeLa cells expressing aequorin targeted to the mitochondrial intermembrane space (mimsAEQ). All conditions as in Fig. 5.

Immunofluorescence data can discriminate the exact localization of mtAEQ within the organelle. To ensure that our $[Ca^{2+}]$ measurements were indeed due to changes in the mitochondrial matrix, we analyzed the effect of uncouplers on measured $[Ca^{2+}]$ levels. Because Ca^{2+} entry into the mitochondrial matrix is made possible by the electrochemical gradient across the IMM, collapse of this gradient with an uncoupler should abolish the changes in $[Ca^{2+}]$ measured by our probe. Using FCCP (5 μM), which dissipates the proton gradient across the IMM, we were unable to detect a significant response to the histamine stimulus, as shown in Fig. 5A. Further confirmation that our probe is indeed localized in the mitochondrial matrix came from experiments with ruthenium red, which is an inhibitor of the calcium uniporter of the IMM. As expected, we were unable to detect a rise in $[Ca^{2+}]_m$ upon stimulation (data not shown).

To determine the relative contribution of each of the two pathways for $[Ca^{2+}]_c$ (i.e., Ca^{2+} release from intracellular stores and Ca^{2+} influx from the extracellular medium), we incubated HeLa cells in a medium without $[Ca^{2+}]$ (with EGTA 100 μM) before histamine stimulation. Under such conditions the increase of the $[Ca^{2+}]_m$ is due only to the release of Ca^{2+} from the intracellular stores. Next, we reintroduced Ca^{2+} into the extracellular medium; in this case the rise in $[Ca^{2+}]_m$ is due to the influx through the plasma membrane channels. Data presented in Fig. 5B show that the release of Ca^{2+} from intracellular stores causes a much larger and faster increase in $[Ca^{2+}]_m$ than the influx through the plasma membrane channels. The larger effect caused by Ca^{2+} relased from the ER suggests that a close proximity between these two organelles could play a key role in the control of mitochondrial Ca^{2+} homeostasis, and thus organelle function.

To test for microdomains of close contact between ER and mitochondria, we constructed a new aequorin chimera, targeted to the IMS (mimsAEQ). Because the OMM is freely permeable to ions and small molecules, aequorin molecules present between the two mitochondrial membranes are located in a region that is in rapid equilibrium with the cytosolic portion in contact with the organelle. Such a chimera is thus sensitive to changes in Ca^{2+} in the region immediately adjacent to mitochondria.

HeLa cells transfected with mimsAEQ and stimulated with histamine show a biphasic response, as shown in Fig. 6. An initial rise in $[Ca^{2+}]_{mims}$ to ~3.5 μM is followed by a rapid decrease, which gradually levels out to values above the initial $[Ca^{2+}]$. As explained previously, this type of response is due to the two mechanisms of action of the agonist: the release of Ca^{2+} from intracellular stores and the entry of Ca^{2+} from the extracellular medium.

Comparison of $[Ca^{2+}]_c$ and $[Ca^{2+}]_{mims}$ responses to histamine shows a clear difference only in the initial phase, which is due to the release of Ca^{2+} from intracellular stores. These data support the hypothesis that the opening of InsP3-sensitive channels in close proximity to mitochondria generates microdomains of high $[Ca^{2+}]$. Indeed, in such microdomains the $[Ca^{2+}]$ is much higher than the average $[Ca^{2+}]_c$. In these circumstances, the low-affinity systems present in mitochondria are capable of accumulating Ca^{2+} in the matrix of the organelle.

To determine the exact location of mimsAEQ, we performed the following experiments. We had previously determined that the collapse of the proton gradient drastically reduces the accumulation of Ca^{2+} in the matrix. If mimsAEQ were localized within the matrix, the rise in $[Ca^{2+}]$ should be abolished in the presence of uncouplers. Conversely, if mimsAEQ were localized in the space between the two mitochondrial membranes, then the presence of uncouplers should not affect the $[Ca^{2+}]$ values obtained. As shown in Fig. 6, HeLa cells transfected with mimsAEQ and treated with FCCP do not show a significant difference in $[Ca^{2+}]$ dynamics when compared to tightly coupled cells, strongly suggesting that the aequorin moiety lies in the IMS.

III. ATP

A. Measuring Free ATP Concentration Dynamically within Mitochondria of Living Cells

In most normal, aerobic cells, mitochondria are the source of the majority of cellular ATP. Thus, knowledge of intramitochondrial ATP concentration, $[ATP]_m$, is of central importance to understanding the bioenergetics of the living cell and its regulation by nutrients, hormones, and other stimuli. Of particular importance is the role of changes in intramitochondrial Ca^{2+} concentration $[Ca^{2+}]_m$ (see earlier discussion), which are likely to activate mitochondrial oxidative metabolism (Denton and McCormack, 1980) through the stimulation of mitochondrial dehydrogenases (Rutter, 1990). Conversely, decreases in ATP concentration within mitochondria may be an important and possibly early event in programmed cell death, resulting from a catastrophic collapse of the mitochondrial membrane potential (Orrenius *et al.*, 1997).

Studies with isolated mitochondria have demonstrated that the free cytosolic and mitochondrial ATP concentrations are likely to be markedly different. Thus, newly synthesized ATP is exported from the mitochondrial matrix electrogenically by ATP^{4-}: ADP^{3-} exchange (LaNoue *et al.*, 1978; Nicholls, 1982). Given a potential of as much as 180 mV across the inner mitochondrial membrane, this is predicted to set values of the ATP/ADP ratio at close to 100 in the cytosol, but nearer to 1.0 in the mitochondrial matrix.

Rapid fractionation techniques (Soboll *et al.,* 1978), applied to hepatocytes and other cell types, have lent support for the existence of this predicted difference in mitochondrial and cytosolic ATP concentration ($[ATP]_c$ and $[ATP]_m$, respectively) in living cells. Here, measurements of total cellular ATP content are made after disruption of the plasma membrane and protein denaturation in acid, using the luciferase activity of *Photinus pyralis* firefly tails (Stanley and Williams, 1969; Soboll *et al.,* 1978). However, such disruptive approaches are fraught with experimental and interpretive difficulties, linked to the inability to determine the *free* ATP concentration within the living cell. Thus, estimates of mitochondrial ATP are confounded by (1) potential contamination with other cellular compartments (e.g., secretory vesicles, lysosomes, Golgi apparatus), (2) binding to proteins and metal ions, and (3) intercellular heterogenity. Hence, measurements of total cellular ATP content provide a limited picture of the dynamic behavior of free [ATP] within mitochondria of a living cell. Further, they provide no information on the subcompartmentalization of mitochondrial ATP, i.e., the free ATP concentration in different mitochondria (or parts of the mitochondrial reticulum) (Rizzuto *et al.,* 1998b).

These problems have led us to search for means by which ATP may be measured dynamically in subcompartments and cytosolic domains of single living cells. One theoretical possibility is the use of ^{31}P-NMR (Scholz *et al.,* 1995). However, this requires large tissue samples and does not provide information on [ATP] changes within cellular organelles. Thus, the potential existence of domains of locally high or low ATP concentration could be missed entirely. Within the cytosol, such domains may exist, e.g., in the vicinity of membranes rich in ATP synthase (i.e., the mitochondrial inner membrane) or rich in ATPase activity (e.g., the plasma Na^+/K^+ ATPase, Ca^{2+} pumps, motor proteins).

At present, then, the best available biosensor for ATP (i.e., one capable of binding the nucleotide and producing a readily detectable signal) has proved to be firefly luciferase. Although purified luciferase protein has been microinjected into cells and used to measure cytosolic free ATP concentration (Bowers *et al.,* 1992), this simple approach precludes targeting of the reporter to the lumen of cellular organelles or its attachment to intracellular membranes. For this, expression of the protein from introduced cDNA is necessary. Firefly luciferase was thus cloned in the late 1980s (De Wet *et al.,* 1987), and versions of the gene, optimized for thermostability and expression in mammalian cells, were generated (Rutter *et al.,* 1998). The enzyme uses an oxidizable substrate, luciferin, which is converted to an AMP adduct before final oxidation and the release of a photon of light (see Fig. 7).

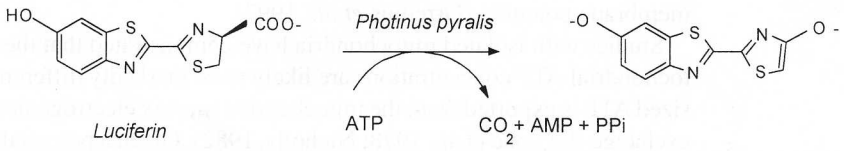

Fig. 7 The ATP-dependent luminescence reaction of luciferase.

B. Dynamic *in Vivo* Measurement of Cytosolic ATP

cDNA encoding luciferase can be introduced readily into most mammalian (and other) cell types by conventional transfection techniques, as discussed for aequorin and GFP, as well as by more sophisticated techniques, including microinjection (Rutter *et al.,* 1995) or the use of adenoviral vectors (see later). While originally intended for detection of the total luciferase amount in cell homogenates, luciferase light output can also be quantitated readily from single living cells, after the addition of the (reasonably cell-permeant) cofactor, luciferin. Under most conditions, O_2 and cofactors other than ATP are not limiting. Further, it can be calculated that the contribution of ATP consumption by luciferase represents only a tiny fraction of total cellular ATP turnover (<0.1%, even at relatively high levels of luciferase expression, e.g., 1×10^6 molecules/cell) and thus nonperturbing for normal cellular ATP homeostasis. Light output from single cells is clearly detectable even after expression from weak promoters, using highly sensitive photon-counting devices and long integration times (minutes) (White *et al.,* 1994; Rutter *et al.,* 1995, 1998; Alekseev *et al.,* 1997).

This technology has been extended to the detection of changes in free intracellular ATP concentration (Kennedy *et al.,* 1999; Jouaville *et al.,* 1999). Here, constitutively high levels of luciferase are expressed from strong viral promoters (e.g., the cytomegalovirus immediate early gene promoter, CMV-IE) so that small fluctuations in free ATP concentrations can be monitored. Relatively rapid imaging (1 data point per 1–10 s) can be performed, most conveniently using the technique of "time-resolved imaging," where the time and location (in 2D) of each single photon event is recorded (Photek, St Leonard's-on-sea, UK). At the single cell level, intensified photon counting cameras perform well (see, *e.g.,* www.photek.co.uk/, photekinc@compuserve.com or Hamamatsu at www.hpk.co.jp/products/producte.htm), although integrating charge-coupled device (CCD) cameras, and even back-illuminated CCD cameras, are usually unable to provide sufficient "detectivity" at physiologically relevant rates of data acquisition. Luciferase-expressing cells are maintained on the microscope stage, and additions are made to the medium in complete darkness. For cell populations, the detection of luciferase luminescence is readily achievable with the photon-counting tube apparatus, as described earlier for the detection of aequorin luminescence (Jouaville *et al.,* 1999; Maechler *et al.,* 1998).

Luciferase displays a K_m for ATP close to 1 m*M* when assayed in cell homogenates under approximate *in vivo* conditions of pH and physiological ionic strength (Kennedy *et al.,* 1999) (compared to the low micromolar range under optimal *in vitro* conditions) (DeLuca *et al.,* 1979). Confirming these values in living cells is complicated due to the distinct kinetics of the enzyme in the living cell ("glow" versus "flash" kinetics). Although the basis for this difference is not fully understood, it may reflect a lack of the accumulation of inhibitory end product (oxyluciferin) in the cell or a decreased sensitivity to this (or other inhibitors) mediated by other cellular cofactors (notably CoA). Whatever the mechanism, this makes monitoring [ATP] constantly in the living cell relatively straightforward, given sensitive photon detection equipment (see earlier discussion). Permeabilization of the cells with digitonin at varying ATP

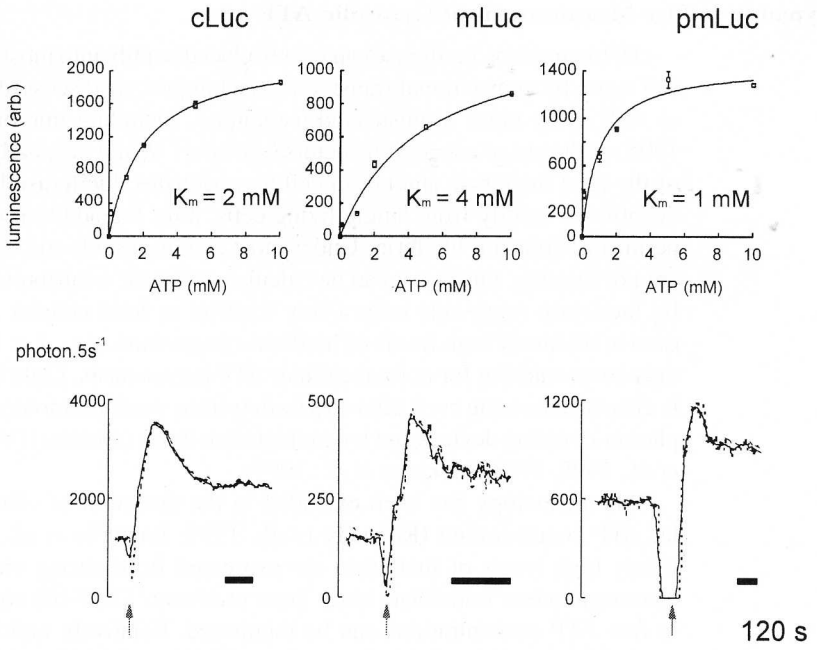

Fig. 8 Calibration of luciferases (*top*) and their use to measure free [ATP] in subcellular compartments of β-cell populations (*bottom*) (from Kennedy *et al.,* 1999). MIN6 β cells were transfected with the constructs shown (c, m, and pm, cytosolic, mitochondrial, and plasma membrane-targeted, respectively) before cell homogenization with detergent and assay of luciferase activity in a conventional luminometer. In the lower traces, luminescence was monitored in intact cells before the addition of digitonin plus a high (10 m*M*) concentration of Mg^{2+}-ATP, to achieve near-saturation of luciferase. Calculated values of [ATP] prior to cell permeabilization were close to 1 m*M* in both cytosolic compartments and the mitochondrial matrix.

concentrations allows calibration of the system and reveals ATP concentrations close to 1 m*M* (Fig. 8) for differently targeted luciferases.

Others (Maechler *et al.,* 1998) have used bacterial toxins to permeabilize cells and perform these calibrations via the addition of progressively increasing concentrations of ATP. However, we have found this a difficult procedure, likely complicated by gradual cell breakage and loss of luciferase. This may account for the discrepancy in K_m values of luciferase for ATP that have been reported (as high as 10 m*M*).

C. Engineering Luciferase for Targeting to Mitochondria

Like aequorin (see earlier discussion), luciferase cDNA can conveniently be fused 3′ to cDNA encoding the mitochondrial import sequence of cytochrome *c* oxidase subunit VIII (Fig. 9). This leads to exclusive mitochondrial localization of the probe (detected with antiluciferase antibodies).

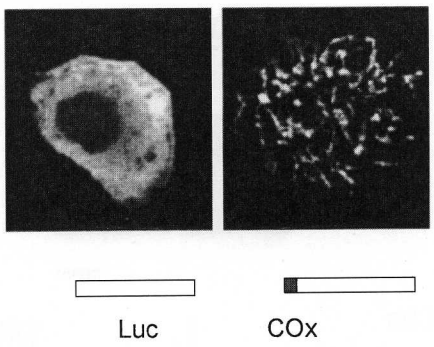

Fig. 9 Immunolocalization of expressed recombinant luciferases within MIN6 islet β cells (from Kennedy *et al.,* 1999). COx, cytochrome *c* oxidase VIII leader, for mitochondrial targeting.

Mitochondrial luciferase displays a very similar K_m value to the cytosolic (untargeted) enzyme, as expected given the removal of the presequence after mitochondrial import. Intriguingly, the free ATP within mitochondria ($[ATP]_m$) was found to be closely similar to that in the cytosol of resting β cells, at around 1.0 m*M* (Fig. 8). This may reflect either (1) a very low mitochondrial membrane potential in the resting cells or (2) a large difference (out < in) in free ADP concentrations, representing a dramatic "phosphorylation potential" in the cytosolic compartment ([ATP]/[ADP]/[Pi]) (LaNoue *et al.,* 1978). It should be stressed that luciferase displays relatively high selectivity for ATP over ADP so that the latter is only a weak inhibitor of activity. As a result, luciferase activity within the cell is likely to report largely [ATP] and not [ATP]/[ADP] ratio (or phosphorylation potential).

Studies with recombinant targeted luciferases have allowed us to monitor changes in free cytosolic ATP concentrations under a number of situations where this is perturbed either by changes in fuel supply to the cell or through cell stimulation with receptor agonists (Kennedy *et al.,* 1999; Jouaville *et al.,* 1999). The latter include hormones that mobilize intracellular Ca^{2+} and alter mitochondrial metabolism via Ca^{2+} accumulation in the mitochondrial matrix and stimulation of intramitochondrial dehydrogenases (Denton and McCormack, 1980; Rutter, 1990). These studies demonstrated that Ca^{2+} increases in the cytosol (and hence mitochondria) are able to activate mitochondrial ATP synthesis, elevating $[ATP]_c$. Strikingly, in the islet β cell, glucose caused much more sustained increases in $[ATP]_m$ than in $[ATP]_c$ (Fig. 10, see color plate). This observation may explain the more sustained increase in [ATP] beneath the plasma membrane, if it is created by localized mitochondria, which are strongly stimulated by locally high Ca^{2+} caused by activated Ca^{2+} influx across the plasma membrane.

Are $[ATP]_m$ changes homogeneous throughout the cell? At present, this question requires greater sensitivity than that achievable with currently available detectors and levels of luciferase expression. Indeed, it has not been possible clearly to resolve single mitochondria nor the mitochondrial reticulum by imaging. Nevertheless, with slower

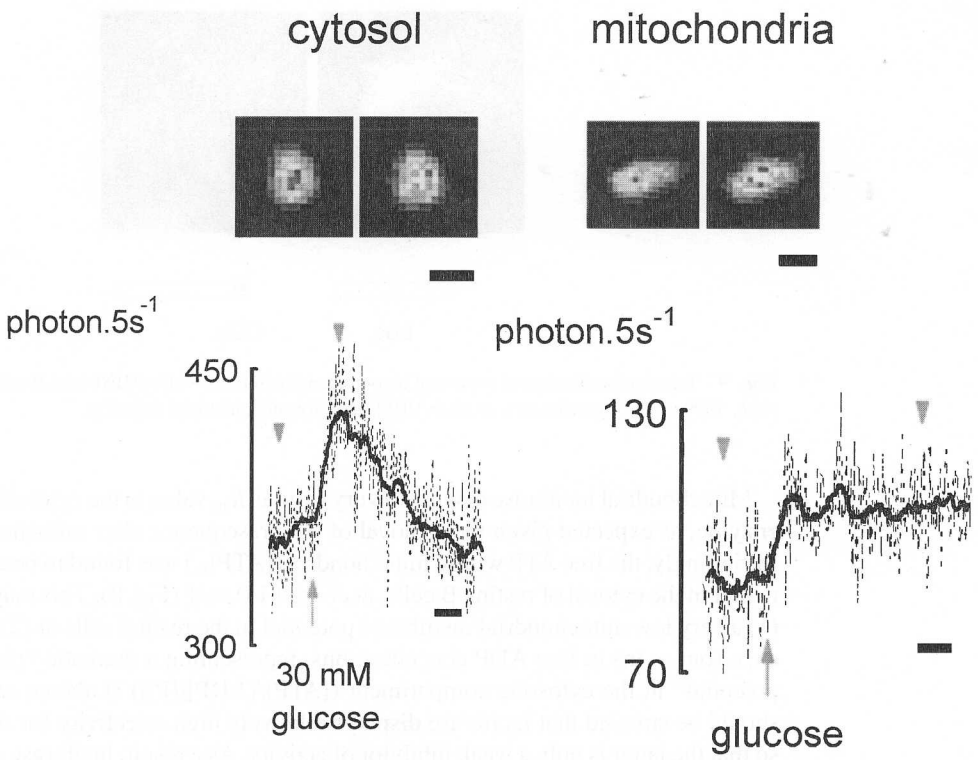

Fig. 10 Glucose-induced changes in free ATP concentration in the cytosol and mitochondrial matrix of MIN6 β cells. Images were produced at the points indicated by the gray arrowheads by integrating photon events over a 30-s interval. Traces show changes recorded from a single cell, with detection of luminescence made every 1 s (broken line) or after integration at each point for 10 s. Scale bar: 5 μm. Time bar: 120 s. From Kennedy *et al.* (1999). Note that individual mitochondria are *not* resolved readily. (See Color Plate.)

data acquisition and improved objective lenses, this may become possible. Similarly, it should be feasible to achieve resolution not only in the x, y but also the z plane. Although confocality is not feasible with a bioluminescent protein (there is no guidable laser, or point of coincidence for multiphoton approaches), digital deconvolution approaches may well become feasible if greater photon detection can be achieved (Rizzuto *et al.*, 1998a).

One potential problem in the use of luciferase is interference from other metabolites. While the concentration of many of these (e.g., phosphate, CoA) changes little or not at all under most conditions, changes in intracellular pH often occur. This may be an especially acute problem with mitochondrial luciferase, as increases in pH enhance luciferase activity, and may occur during the activation of mitochondrial dehydrogenases and the respiratory chain during increases in intracellular [Ca^{2+}]. Molecular engineering

of luciferase, whose 3D structure was solved to 2.8 Å (Conti *et al.,* 1996) may offer approaches to address this problem.

D. Generating and Using Adenoviral Luciferase Vectors

A limitation of the use of expressed luciferases is that of achieving both adequate efficiency of transfection (2–10% is normal with conventional procedures) and adequate levels of expression in individual cells. Further, many cell types (especially primary cells) are difficult to transfect by conventional means (Ca-phosphate, lipoamines, electroporation, etc.). For this reason, much interest has shifted to the use of retro- and, more particularly, replication-deficient adenoviruses as a means of DNA introduction. The latter are particularly attractive, as >95% of cells of *any* mammalian species/embryological origin can typically be infected by low (entirely nontoxic) viral titers. This is also especially valuable for the study of intact organs, microorgans (e.g., islet β cells), or tissue slices (e.g., hippocampal neuron cultures), where conventional transfection is essentially impossible. For example, the power of this approach is revealed by the fact that >90% of cells within an intact pancreatic islet (a spherical microorgan of diameter approximately 200 μm) are rapidly infected to express GFP or luciferase. Furthermore, measurements of ATP using luciferase within the intact animal are in principle feasible (and luciferase has been imaged in living transgenic mice, albeit with relatively long integration times and sedated animals; Contag *et al.,* 1998). The procedure for adenoviral synthesis has been enhanced greatly with the ability to perform homologous recombination within bacteria (He *et al.,* 1998). It should now be possible to generate adenoviral versions of both cytosolic and mitochondrially targeted luciferase with which to address a range of biological questions in a range of primary cell types.

E. Future Prospects for the Use of Mitochondrially Targeted Luciferases

Targeted recombinant luciferase represents a dramatic advance in the ability to measure ATP dynamically and *in vivo* and in single cells. Although we have focused largely on the use of this tool to measure ATP concentration within the cytosol or the mitochondrial lumen, exploration of further mitochondrial subdomains may well yield surprises about mitochondrial function. For example, how does [ATP] change in the intermembrane space or at the surface of the outer mitochondrial membrane and is there a gradient between these two "compartments"? Indeed, luciferase has already been targeted to the OMM in yeast cells (Aflalo, 1990), but no measurements have yet been made in higher eukaryotes. Is the concentration of ATP the same in the "bulk" mitochondrial matrix as it is immediately beneath the mitochondrial inner membrane? Is it feasible to make multiple simultaneous recordings from luciferases (e.g., with altered luminescence spectra) and targeted to different domains or to image luciferase simultaneously with other fluorescent or luminescent reporters (such as aequorin)? These questions should be addressed in the near future given the targeting, gene delivery, and low light level imaging technologies now in existence. Other details are available at http://www.bch.bris.ac.uk/staff/rutter/index.html.

IV. pH

A. Intracellular pH

Intracellular pH (pH_i) regulates many cellular processes, including cell metabolism (Roos and Boron, 1981), gene expression (Isfort *et al.,* 1993) cell–cell coupling (Orchard and Kentish, 1990), cell adhesion (Tominga *et al.,* 1998), and cell death (Gottlied *et al.,* 1996).

The pH-sensitive fluorochromes 2′,7′-bis(carboxyethyl)-5,6-carboxyfluorescein (BCECF) and the most recently developed carboxyseminaphthorhodafluor-1 (SNARF1) and 5′,6′-carboxy seminaphthofluorescein (SNAFL) have been widely employed to monitor pH_i in both cell populations and single cells. These probes, synthesized as acetoxymethyester derivatives, are cell permeant and have the property to shift their light emission or excitation spectrum as a function of pH. Moreover, excitation wavelengths of SNARF and SNAFL enable their use with a laser confocal microscope (Zhou *et al.,* 1995). Measurements of pH_i with these dyes present some problems: during the course of experiments a significant leakage of the pH indicator occurs, which can be considerable in cells incubated at 37°C. In addition, some cells are resistant to loading because of physical barriers, such as a cell wall (bacteria, yeast, and plants) or the thickness of the tissue preparation. The most important limitation of the use of these compounds is that pH_i measurements are restricted to the cytosol and nucleus, whereas pH changes occurring in other intracellular organelles cannot be directly determined in intact cells.

This restriction is prominent for organelles such as mitochondria and the Golgi, where a proton gradient is built up by specific H^+ transport mechanisms. In mitochondria, it is universally accepted that the H^+ electrochemical potential ($\Delta\mu_{H+}$), generated by electron transport across the inner membrane coupled to H^+ ejection on the redox H^+ pumps, is used to drive ATP synthesis by ATP-synthase. In addition to ATP synthesis, $\Delta\mu_{H+}$ supports a variety of mitochondrial processes, some of which are a prerequisite for respiration and ATP synthesis, such as (1) uptake of respiratory substrates and phosphate, of ADP in exchange for ATP, and of Ca^{2+} ions; (2) the transhydrogenation reaction, and (3) the import of respiratory chain and ATP synthase subunits encoded by nuclear genes. $\Delta\mu_H^+$ comprises both the electrical ($\Delta\psi$) and the chemical component of the H^+ gradient (ΔpH). It is well established that under physiological conditions, $\Delta\psi$ represents the dominant component of $\Delta\mu_H^+$, whereas the ΔpH gradient is small. The relative contribution of $\Delta\psi$ and ΔpH across the mitochondrial membrane can be changed by the redistribution of permeant ions, such as phosphate, Ca^{2+}, or K^+, in the presence of the ionophore valinomycin. Several techniques have been developed for the determination of $\Delta\psi$ and ΔpH in isolated mitochondria (Nicholls and Fergusson, 1992). Attempts have also been carried out to measure $\Delta\psi_m$ in intact cells [for a critical evaluation of these methods, see Bernardi *et al.* (1999)]. However, measurements of matrix pH have been elusive due to the difficulty of separating the mitochondrial signal from its surrounding cytoplasm (Chacon *et al.,* 1994).

One of the most promising tools developed to overcome this difficulty is the use of recombinant pH-sensitive fluorescent proteins targeted specifically to the mitochondrial compartments.

B. pH-Sensitive Fluorescent Proteins

The GFP from *A. victoria* has been widely used as a noninvasive fluorescent reporter for gene expression (Chalfie *et al.,* 1994), protein localization (Rizzuto *et al.,* 1995), and protein trafficking (Pines, 1995). Its small size (approximately 27 kDa) and its ability to retain its intrinsic fluorescence when fused with other peptides have made GFP a very useful tool for cellular biology studies (Tsien, 1998).

Structural analysis by X-ray crystallography revealed that the cylindrical fold of GFP is made up of an 11-stranded β-barrel, threaded by an α-helix running up the axis of the cylinder. The chromophore is attached to the α-helix and is buried in the center of the cylinder. The chromophore is formed from residues 65–67, which are Ser-Tyr-Gly in the native protein, which undergo intramolecular autocatalytic cyclization and oxidation (Ormö *et al.,* 1996).

The *in vitro* spectral characteristics of both purified and recombinant wild-type GFP and of a number of other GFP mutants are influenced by pH, suggesting a pH; sensing activity for this class of proteins (Ward and Bokman, 1982; Patterson *et al.,* 1997). Therefore, the possibility has been explored that GFP mutants might be used as a pH sensor in living cells. This possibility was first investigated by Kneen *et al.* (1998), who reported that mutations S65T and F64L/S65T of wild-type GFP exhibited indistinguishable fluorescent spectra and pH titration data, with a pK_a value of 5.98. The pH-dependent absorbance spectrum of *in vitro* S65T-GFP is reported in Fig. 11A. It is apparent that the peak at 490 nm increased from pH 4 to 7.5. The finding that the titration curve for S65T-GFP was similar to that of fluorescein suggested the involvement of a single amino acid residue in its pH-sensitive mechanism (Kneen *et al.,* 1998). Crystallographic analysis of this GFP mutant at both basic (pH 8.0) and acidic (pH 4.6) pH, identify a model, likely

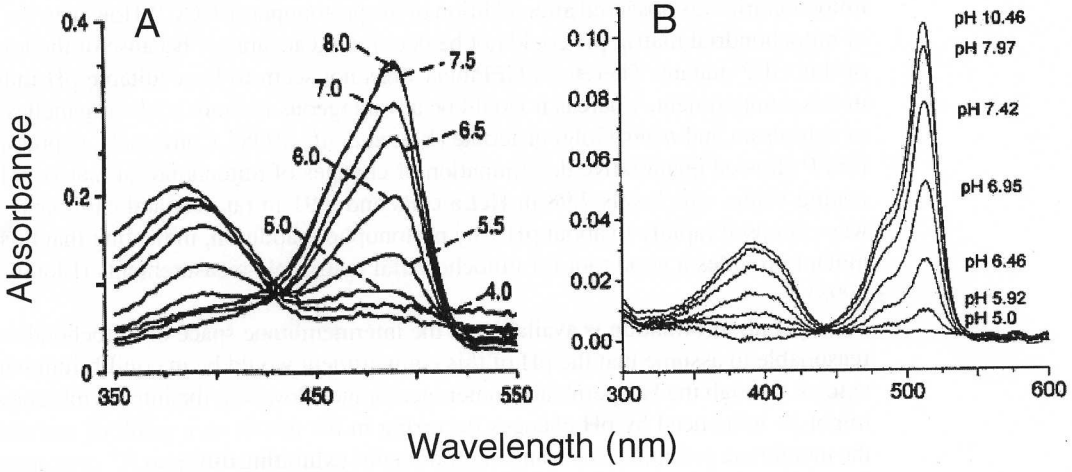

Fig. 11 pH-dependent absorbance spectra of purified S65T-GFP (A) and EYFP (B), modified from Kneen *et al.* (1998) and Llopis *et al.* (1998), respectively.

valid for other mutants as well, where the phenolic hydroxyl deriving from Tyr66 is the site of protonation (Elsliger *et al.,* 1999).

The same GFP mutant (F64L/S65T), termed GFPmut1, was expressed heterologously in the cytosol and nuclear compartments of BS-C-1 cells or rabbit proximal tubule cells. In this study, comparison of GFPmut1 and the pH-sensitive dye BCECF has been carried out, showing uniform agreement between pH_i estimates with the two methods (Robey *et al.,* 1998).

Another pH-sensitive GFP mutant, called enhanced yellow fluorescent protein (EYFP), was made by introducing the amino acid substitutions S65G/S72A/T203Y. The absorbance spectrum of EYFP *in vitro* is reported in Fig. 11B, showing that the absorbance of the peak at 514 nm increased from pH 5 to 8 (Llopis *et al.,* 1998). The apparent pK_a value of 7.1 suggests that this protein should be suitable for pH_i measurements in most subcellular compartments, particularly in the mitochondrial matrix, which is expected to be alkaline.

C. Mitochondrial-Targeted pH-Sensitive GFP

1. Available GFP Chimeras

We currently employ as pH sensors two targeted versions of the GFP mutant (S65G/S72A/T203Y), described earlier. The first is targeted to the mitochondrial matrix (mtYFP) by fusion to the targeting sequence of COX8. As Tsien (1998) described, a matrix-targeted chimera is appropriately sorted and faithfully reports the pH changes of this domain. The suitability of these GFP mutants as pH indicators in the mitochondrial matrix of living cells was evaluated in CHO (Kneen *et al.,* 1998), in HeLa cells, and in rat neonatal cardiomyocytes (Llopis *et al.,* 1998). In CHO cells expressing recombinant GFPmut1 targeted to the mitochondrial matrix, a qualitative reversible acidification of mitochondria was observed after addition of the protonophore CCCP. However, the value of mitochondrial matrix pH could not be determined accurately because of the low pK_a of this GFP mutant. Therefore, GFPmut1 does not seem to be a suitable pH indicator in this compartment, whereas it would be advantageous in more acidic organelles, such as cytoplasm and *trans*-Golgi cisternae (Kneen *et al.,* 1998). Conversely, expression of EYFP allowed quantitative determination of changes of mitochondrial matrix pH. The resting value, which was 7.98 in HeLa cells and 7.91 in rat neonatal cardiomyocytes, was collapsed rapidly to about pH 7 by protonophore addition, indicating that this GFP mutant provides a good tool for mitochondrial matrix pH measurements (Llopis *et al.,* 1998).

As yet no information is available on the intermembrane space of mitochondria. It is reasonable to assume that the pH of this compartment would be in equilibrium with the cytosol through the H^+-permeable outer membrane. However, the intermembrane space might be influenced by pH changes occurring in the matrix as a result of variations in the membrane potential ($\Delta\psi$), and microdomains exhibiting different H^+ concentrations from cytosol might exist under physiological and pathological conditions. During the process of apoptosis, for instance, the intermembrane space likely undergoes a dramatic

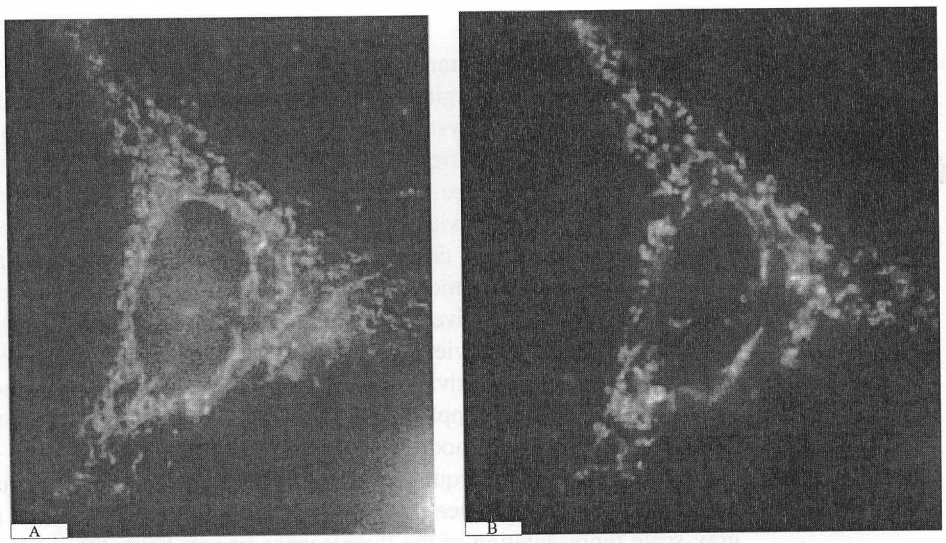

Fig. 12 HeLa cells expressing MIMS-EYFP and clamped at pH 6.5 (A) and 7.5 (B). Cells were observed 36 h after transfection using a back-illuminated CCD camera (Princeton Instruments) and Metamorph software (Universal Imaging).

change, as a few proteins normally resident in this compartment, such as cytochrome *c* and "apoptosis inducing factor," are released into the cytoplasm, where they play a crucial role in the effector phase of cell death.

EYFP targeted to the IMS has been constructed using the same cloning strategy employed for MIMS-targeted aequorin (Pinton *et al.*, 1998a). Transfection of HeLa cells with mimsEYFP yields the typical pattern of mitochondrial labeling, as shown in the image reported in Fig. 12, obtained with a digital imaging microscope (Rizzuto *et al.*, 1998a).

D. Detecting and Calibrating the Signal of Targeted GFP Mutants

1. Recombinant Expression

The procedures employed for expressing mtEYFP and mimsEYFP are the same as those described previously for the corresponding aequorin and luciferase chimeras, i.e., in most cases a simple transfection via the calcium phosphate protocol. The only difference is that the cells are seeded onto a 25-mm coverslip and transfected with 8 μg DNA/coverslip. In the case of mimsEYFP, the amount of DNA can be reduced to 2–4 μg/coverslip to prevent mitochondrial damage. It is our experience that in many cell types high levels of expression of a recombinant protein retained in the IMS (i.e., not only YFP, but also aequorin; see earlier discussion) cause a morphological rearrangement of mitochondria.

2. Visualizing GFP

Thirty-six hours after transfection the coverslip with the cells is transferred to the thermostatted stage of a digital imaging system, as described previously (Rizzuto *et al.*, 1998a). We describe our systems here briefly, but obviously the setup can be assembled with similar components from different manifacturers. Our two setups are composed of an inverted fluorescence microscope (a Nikon Eclipse 300 and a Zeiss Axiovert), an excitation filter wheel with shutter from Sutter Instruments, the dedicated YFP filter sets of Chroma (however, comparable results can be obtained with a traditional FITC set), a back-illuminated camera from Princeton Instruments, and the acquisition/analysis software Metafluor of Universal Imaging. For each time point, the fluorescence image from the selected field of view and the fluorescence intensity of the region(s) of interest can be obtained. The sensitivity of the camera results in reduction of the time of exposure to 50–100 ms in many applications. Under these conditions, prolonged experiments can be carried out with modest bleaching of the fluorophore (e.g., <20% in a 5-min experiment with image acquisition at 1- to 2-s intervals). Throughout the experiment, the variation in fluorescence intensity caused by agonists and drugs is revealed by the gray-scale representation of the fluorescence image. From the images of the same cell clamped at pH 6.5 and pH 7.5, shown in Fig. 12, it is apparent that the fluorescence signal increases with pH.

3. Converting the YFP Signal into pH Values

Coverslips with mimsEYFP-transfected cells were mounted in the thermostatted chamber (37°C) and incubated in a KCl-based saline solution containing 125 m*M* KCl, 20 m*M* NaCl, 5.5 m*M* D-glucose, 1 m*M* $CaCl_2$, 1 m*M* $MgSO_4$, 1 m*M* K_2HPO_4, 20 m*M* Na-HEPES (pH 6.5), and the ionophores nigericin and monensin (5 μM) to equalize intracellular and extracellular pH. pH was increased by additions of small amounts of NaOH while measuring the pH with a semimicrombination pH electrode. mimsEYFP fluorescence in selected areas of cells was linear with pH over the range between pH 6.5 and 8, with a linear regression coefficient between 0.9 and 0.97 in three experiments.

Quantitative determination of fluorescence in selected areas of cells as a function of pH allowed construction of the titration curve shown in Fig. 13. The estimated pH value in the IMS of HeLa cells was 7.21 ± 0.15 (six cells from three experiments), which is close to the pH_i value of 7.31 ± 0.2 (four cells from two experiments) determined with EYFP targeted to the cytosol (not shown).

V. Conclusion

Two powerful tools are now available to monitor the changes in pH in the mitochondrial intermembrane space and the matrix *in situ* in intact cells, and the relationship existing between the pH of these compartments and that of the cytosol. These probes have the great advantage of being specifically targeted to the two mitochondrial compartments and,

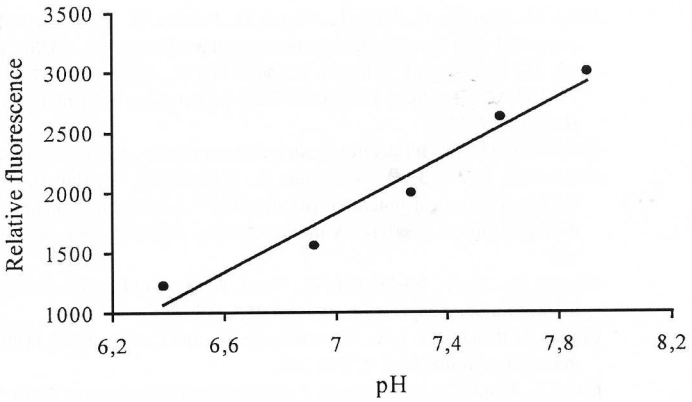

Fig. 13 *In situ* titration curve of MIMS-EYFP fluorescence as a function of pH. The curve is representative of three experiments.

through use of digital fluorescence microscopy, allow acquisition of three-dimensional images of cells in real time and with high spatial resolution. It would be possible to assess whether some regions of the mitochondrial matrix are more active than others in H^+ translocation or whether pH gradients or changes are present in the intermembrane space during cell activation by cell surface receptors or during the onset of apoptosis. The stability of these proteins and their lack of toxicity make them ideal visual indicators for a wide array of cellular applications *in vivo*.

Acknowledgments

We gratefully acknowledge grant support from Telethon, the Italian University and Health Ministries to R.R., from the Medical Research Council, U.K. (Post doctoral Fellowship to E.K.A., and the Bristol MRC Cell Imaging Facility), the Biotechnology and Biological Sciences Research Council, British Diabetic Association, and Wellcome Trust to E.K.A. and G.R. and from PRIN "Bionergetica e trasporto di membrana" to A.M.P. and M.R.

References

Aflalo, C. (1990). Targeting of cloned firefly luciferase to yeast mitochondria. *Biochemistry* **29,** 4758–4766.

Alekseev, A. E., Kennedy, M. E., Navarro, B., and Terzic, A. (1997). Burst kinetics of co-expressed Kir6.2/SUR1 clones: Comparison of recombinant with native ATP-sensitive K^+ channel behavior. *J. Membr. Biol.* **159,** 161–168.

Bernardi, P., Scorrano, L., Colonna, R., Petronilli, V., and Di Lisa, F. (1999). Mitochondrial and cell death: Mechanistic aspects and methodological issues. *Eur. J. Biochem.* **264,** 687–701.

Bowers, K. C., Allshire, A. P., and Cobbold, P. H. (1992). Bioluminescent measurement in single cardiomyocytes of sudden cytosolic ATP depletion coincident with rigor. *J. Mol. Cell Cardiol.* **24,** 213–218.

Brini, M., Marsault, R., Bastianutto, C., Alvarez, J., Pozzan, T., and Rizzuto, R. (1995). Transfected aequorin in the measurement of cytosolic Ca^{2+} concentration ($[Ca^{2+}]_c$): A critical evaluation. *J. Biol. Chem.* **270,** 9896–9903.

Brini, M., Murgia, M., Pasti, L., Picard, D., Pozzan, T., and Rizzuto, R. (1993). Nuclear Ca^{2+} concentration measured with specifically targeted recombinant aequorin. *EMBO J.* **12,** 4813–4819.

Brini, M., De Giorgi, F., Murgia, M., Marsault, R., Massimino, M. L., Cantini, M., Rizzuto, R., and Pozzan, T. (1997). Subcellular analysis of Ca^{2+} homeostasis in primary cultures of skeletal myotubes. *Mol. Cell. Biol.* **8,** 129–143.

Carafoli, E. (1987). Intracellular calcium homeostasis. *Annu. Rev. Biochem.* **56,** 395–433.

Chacon, E., Reece, J. M., Nieminen, A., Zahrebelski, G., Herman, B., and Lemasters, J. J. (1994). Distribution of electrical potential, pH, free Ca^{2+}, and volume inside cultured adult rabbit cardiac myocytes during chemical hypoxia: A multiparameter digitized confocal microscopic study. *Biophys. J.* **66,** 942–952.

Chalfie, M., Tu, Y., Euskirchen, G., Ward, W. W., and Prasher, D. C. (1994). Green fluorescent protein as a marker for gene expression. *Science* **263,** 802–805.

Contag, P. R., Olomu, I. N., Stevenson, D. K., and Contag, C. H. (1998). Bioluminescent indicators in living mammals. *Nature Med.* **4,** 245–247.

Conti, E., Franks, N. P., and Brick, P. (1996). Crystal structure of firefly luciferase throws light on a superfamily of adenylate-forming enzymes. *Structure* **4,** 287–298.

DeLuca, M., Wannlund, J., and McElroy, W. D. (1979). Factors affecting the kinetics of light emission from crude and purified firefly luciferase. *Anal. Biochem.* **95,** 194–198.

Denton, R. M., and McCormack, J. G. (1980). On the role of the calcium transport cycle in the heart and other mammalian mitochondria. *FEBS Lett.* **119,** 1–8.

De Wet, J. R., Wood, K. V., and DeLuca, M., *et al.* (1987). Firefly luciferase gene: Structure and expression in mammalian cells. *Mol. Cell. Biol.* **7,** 725–737.

Elsliger, M.-A., Wachter, R. M., Hanson, G. T., Kallio, K., and Remington, S. J. (1999). Structural and spectral response of green fluorescent protein variants to changes in pH. *Biochemistry* **38,** 5296–5301.

Gottlieb, R. A., Grauol, D. L., Zhu, J. Y., and Engler, R. L. (1996). Preconditioning rabbit cardiomyocytes: Role of pH, vacuolar proton ATPase and apoptosis. *J. Clin. Invest.* **97,** 2391–2398.

Gunter, K. K., and Gunter, T. E. (1994). Transport of calcium by mitochondria. *J. Bioenerg. Biomembr.* **26,** 471–485.

Halestrap, A. P. (1989). The regulation of the matrix volume of mammalian mitochondria in vivo and in vitro and its role in the control of mitochondrial metabolism. *Biochim. Biophys. Acta* **973,** 355–382.

He, T. C., Zhou, S., da Costa, L. T., Yu, J., Kinzler, K. W., and Vogelstein, B. (1998). A simplified system for generating recombinant adenoviruses. *Proc. Natl. Acad. Sci. USA* **95,** 2509–2514.

Isfort, R. J., Cody, D. B., Asquith, T. N., Ridder, G. M., Stuard, S. B., and LeoBoeuf, R. A. (1993). Induction of protein phosphorylation, protein synthesis: Immediate-early-gene expression and cellular proliferation by intracellular pH modulation. Implications for the role of hydrogen ions in signal transduction. *Eur. J. Biochem.* **213,** 349–357.

Jouvaille, L. S., Pinton, P., Bastianutto, C., Rutter, G. A., and Rizzuto, R. (1999). Regulation of mitochondrial ATP synthesis by calcium: Evidence for a long-term metabolic priming. *Proc. Natl. Acad. Sci. USA* **96,** 13807–13812.

Kennedy, H. J., Pouli, A. E., Jouvaille, L. S., Rizzuto, R., and Rutter, G. A. (1999). Glucose-induced ATP microdomains in single islet beta-cells. *J. Biol. Chem.* **274,** 13281–13291.

Kneen, M., Farinas, J., Li, Y., and Verkman, A. S. (1998). Green fluorescent protein as a noninvasive intracellular pH indicator. *Biophys. J.* **74,** 1591–1599.

LaNoue, K., Mizani, S. M., and Klingenberg, M. (1978). Electrical imbalance of adenine nucleotide transport across the mitochondrial membrane. *J. Biol. Chem.* **253,** 191–198.

Llopis, J., McCaffery, J. M., Miyawaki, A., Farquhar, M., and Tsien, R. Y. (1998). Measurement of cytosolic, mitochondrial, and Golgi pH in single living cells with green fluorescent proteins. *Proc. Natl. Acad. Sci. USA* **95,** 6803–6807.

Maechler, P., Wang, H., and Wollheim, C. B. (1998). Continuous monitoring of ATP levels in living insulin secreting cells expressing cytosolic firefly luciferase. *FEBS Lett.* **422,** 328–332.

Marsault, R., Murgia, M., Pozzan, T., and Rizzuto, R. (1997). Domains of high Ca^{2+} beneath the plasma membrane of living A7r5 cells. *EMBO J.* **16,** 1575–1581.

Montero, M., Brini, M., Marsault, R., Alvarez, J., Sitia, R., Pozzan, T., and Rizzuto, R. (1995). Monitoring dynamic changes in free Ca^{2+} concentration in the endoplasmic reticulum of intact cells. *EMBO J.* **14,** 5467–5475.

Nicholls, D. G. (1982). "Bioenergetics: An Introduction to the Chemiosmotic Theory." Academic Press, London

Nicholls, D. G., and Fergusson, S. F. (1992). Quantitative bioenergetics: The measurements of driving forces *In* "Bioenergetics 2," p. 39–63. Academic Press, London

Orchard, C. H., and Kentish, J. C. (1990). Effects of changes of pH on the contractile function of cardiac muscle. *Am. J. Physiol.* **258,** C967–C981.

Ormö, M., Cubitt, A. B., Kallio, Gross, L. A., Tsien, R. Y., and Remington, S. J. (1996). Crystal structure of the *Aequorea victoria* green fluorescent protein. *Science* **273,** 1392–1395.

Orrenius, S., Burgess, D. H., Hampton, M. B., and Zhivotovsky, B. (1997). Mitochondira as the focus of apoptosis research. *Cell Death Differ.* **4,** 427–428.

Patterson, G. H., Knobel, S. M., Sharif, W. D., Kain, S. R., and Piston, D. W. (1997). Use of the green fluorescent protein and its mutants in quantitative fluorescence microscopy. *Biophys. J.* **73,** 2782–2790.

Pines, J. (1995). GFP in mammalian cells. *Trends Genet.* **11,** 326–327.

Pinton, P., Brini, M., Bastianutto, C., Tuft, R. A., Pozzan, T., and Rizzuto, R. (1998a). New light on mitochondrial calcium. *BioFactors* **8,** 243–253.

Pinton, P., Pozzan, T., and Rizzuto., R. (1998b). The Golgi apparatus is an inositol 1,4,5 trisphosphate Ca^{2+} store, with distinct functional properties from the endoplasmic reticulum. *EMBO J.* **18,** 5298–5308.

Pozzan, T., Rizzuto, R., Volpe, P., and Meldolesi, J. (1994). Molecular and cellular physiology of intracellular Ca^{2+} stores. *Physiol. Rev.* **74/3,** 595–636.

Rizzuto, R., Brini, M., Murgia, M., and Pozzan, T. (1993). Microdomains of cytosolic Ca^{2+} concentration sensed by strategically located mitochondria. *Science* **262,** 744–747.

Rizzuto, R., Brini, M., Pizzo, P., Murgia, M., and Pozzan, T. (1995). Chimeric green fluorescent protein: A new tool for visualizing subcellular organelles in living cells. *Curr. Biol.* **5,** 635–642.

Rizzuto, R., Carrington, W., and Tuft, R. A. (1998a). Digital imaging microscopy of living cells. *Trends Cell Biol.* **8,** 288–292.

Rizzuto, R., Pinton, P., Carrington, W., Fay, F. S., Fogarty, K. E., Lifshitz, L. M., Tuft, R. A., and Pozzan, T. (1998b). Close contacts with the endoplasmic reticulum as determinants of mitochondrial Ca^{2+} responses. *Science* **280,** 1763–1766.

Rizzuto, R., Simpson, A. W. M., Brini, M., and Pozzan, T. (1992). Rapid changes of mitochondrial Ca^{2+} revealed by specifically targeted recombinant aequorin. *Nature* **358,** 325–328.

Robb-Gaspers, L. D., Burnett, P., Rutter, G. A., Denton, R. M., Rizzuto, R., and Thomas, A. P. (1998). Integrating cytosolic calcium signals into mitochondrial metabolic responses. *EMBO J.* **17,** 4987–5000.

Robey, R. B., Ruiz, O., Santos, A. V. P., Ma, J., Kear, F., Wang, L.-J., Li, C.-J., Bernardo, A. A., and Arruda, J. A. L. (1998). pH-dependent fluorescence of a heterologously expressed *Aequorea* green fluorescent protein mutant: In situ spectral characteristics and applicability to intracellular pH estimation. *Biochemistry* **37,** 9894–9901.

Roos, A., and Boron, W. F. (1981). Intracellular pH. *Physiol. Rev.* **61,** 296–434.

Rutter, G. A. (1990). Ca^{2+}-binding to citrate cycle enzymes. *Int. J. Biochem.* **22,** 1081–1088.

Rutter, G. A., Burnett, P., Rizzuto, R., Brini, M., Murgia, M., Pozzan, T., Tavaré, J. M., and Denton, R. M. (1996). Subcellular imaging of intramitochondrial Ca^{2+} with recombinant targeted aequorin: Significance for the regulation of pyruvate dehydrogenase activity. *Proc. Natl. Acad. Sci. USA* **93,** 5489–5494.

Rutter, G. A., Kennedy, H. J., Wood, C. D., White, M. R. H., and Tavare, J. M. (1998). Quantitative realtime imaging of gene expression in single cells using multiple luciferase reporters. *Chem. Biol.* **5,** R285–R290. [Abstract]

Rutter, G. A., Theler, J. M., Murgia, M., Wollheim, C. B., Pozzan, T., and Rizzuto, R. (1993). Stimulated Ca^{2+} influx raises mitochondrial free Ca^{2+} to supramicromolar levels in a pancreatic β-cell line. *J. Biol. Chem.* **268,** 22385–22390.

Rutter, G. A., White, M. R. H., and Tavare, J. M. (1995). Non-invasive imaging of luciferase gene expression in single living cells reveals the involvement of MAP kinase in insulin signalling. *Curr. Biol.* **5,** 890–899.

Scholz, T. D., Laughlin, M. R., Balaban, R. S., Kupriyanov, V. V., and Heineman, F. W. (1995). Effect of substrate on mitochondrial NADH, cytosolic redox state, and phosphorylated compounds in isolated hearts. *Am. J. Physiol.* **268,** H82–H91.

Soboll, S., Scholz, R., and Heldt, H. W. (1978). Subcellular metabolite concentrations: Dependence of mitochondrial and cytosolic ATP systems on the metabolic state of perfused rat liver. *Eur. J. Biochem.* **87,** 377–390.

Stanley, P. E., and Williams, S. G. (1969). Use of the liquid scintillation spectrometer for determining adenosine triphosphate by the luciferase enzyme. *Anal. Biochem.* **29,** 381–392.

Tsien, R. Y. (1998). The green fluorescent protein. *Annu. Rev. Biochem.* **67,** 509–544.

Ward, W. W., and Bokman, S. H. (1982). Reversible denaturation of *Aequorea* green fluorescent protein: Physical separation and characterization of the renatured protein. *Biochemistry* **21,** 4535–4540.

White, M. R. H., Masuko, M., Amet, L., Elliott, G., Braddock, M., Kingsman, A. J., and Kingsman, S. M. (1994). Real-time analysis of the transcriptional regulation of HIV and hCMV promoters in single mammalian cells. *J. Cell Sci.* **108,** 441–455.

Zhou, Y., Marcus, E. M., Haugland, R. P., and Opas, M. (1995). Use of a new fluorescent probe, seminaphthofluorescein-calcein, for determination of intracellular pH by simultaneous dual-emission imaging laser scanning confocal microscopy. *J. Cell Physiol.* **146,** 9–16.

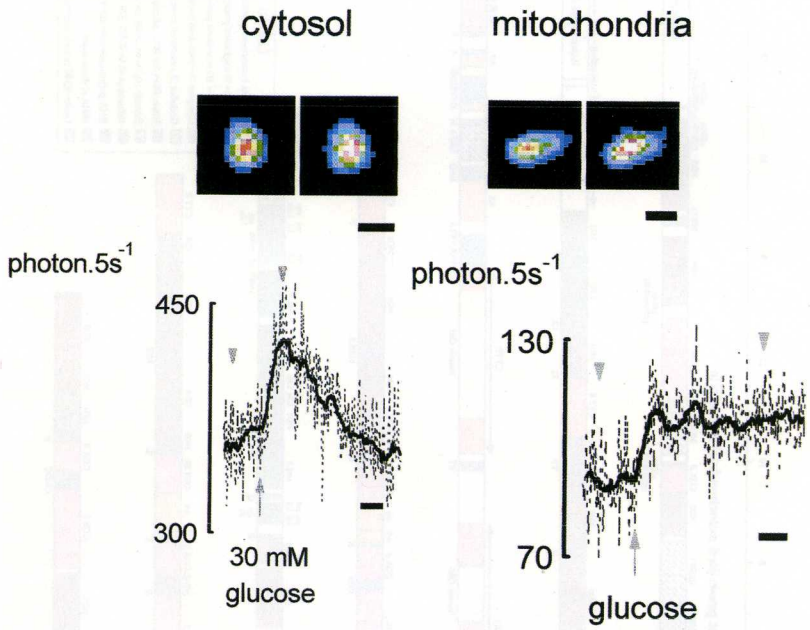

Fig. 20.10 Glucose-induced changes in free ATP concentration in the cytosol and mitochondrial matrix of MIN6 β cells. Images were produced at the points indicated by the gray arrowheads by integrating photon events over a 30-s interval. Traces show changes recorded from a single cell, with detection of luminescence made every 1 s (broken line) or after integration at each point for 10 s. Scale bar: 5μm Time bar: 120 s. From Kennedy *et al.* (1999). Note that individual mitochondria are *not* resolved readily.